Synergy between Piezo1 and Piezo2 channels confers high-strain mechanosensitivity to articular cartilage

Whasil Lee[a], Holly A. Leddy[b], Yong Chen[a], Suk Hee Lee[a], Nicole A. Zelenski[b], Amy L. McNulty[b], Jason Wu[c], Kellie N. Beicker[d], Jeffrey Coles[e], Stefan Zauscher[e], Jörg Grandl[c], Frederick Sachs[f], Farshid Guilak[b,e,1], and Wolfgang B. Liedtke[a,c,g,1]

Departments of [a]Neurology, [b]Orthopaedic Surgery, and [c]Neurobiology, and [g]Clinics for Pain and Palliative Care, Duke University Medical Center, Durham, NC 27710; [e]Department of Mechanical Engineering and Materials Science, Duke University, Durham, NC 27708; [d]Department of Physics and Astronomy, University of North Carolina at Chapel Hill, Chapel Hill, NC 27599; and [f]Department of Physiology and Biophysics, State University of New York, Buffalo, NY 14214

Edited by Richard W. Aldrich, The University of Texas at Austin, Austin, TX, and approved October 15, 2014 (received for review July 28, 2014)

Diarthrodial joints are essential for load bearing and locomotion. Physiologically, articular cartilage sustains millions of cycles of mechanical loading. Chondrocytes, the cells in cartilage, regulate their metabolic activities in response to mechanical loading. Pathological mechanical stress can lead to maladaptive cellular responses and subsequent cartilage degeneration. We sought to deconstruct chondrocyte mechanotransduction by identifying mechanosensitive ion channels functioning at injurious levels of strain. We detected robust expression of the recently identified mechanosensitive channels, PIEZO1 and PIEZO2. Combined directed expression of Piezo1 and -2 sustained potentiated mechanically induced Ca^{2+} signals and electrical currents compared with single-Piezo expression. In primary articular chondrocytes, mechanically evoked Ca^{2+} transients produced by atomic force microscopy were inhibited by GsMTx4, a PIEZO-blocking peptide, and by Piezo1- or Piezo2-specific siRNA. We complemented the cellular approach with an explant-cartilage injury model. GsMTx4 reduced chondrocyte death after mechanical injury, suggesting a possible therapy for reducing cartilage injury and posttraumatic osteoarthritis by attenuating Piezo-mediated cartilage mechanotransduction of injurious strains.

cartilage | chondrocyte | mechanotransduction | cartilage injury | Piezo

Articular cartilage is a hydrated connective tissue that supports loads and minimizes friction in the diarthrodial joints. It has a highly differentiated extracellular matrix (ECM) composed primarily of type II collagen, the large aggregating proteoglycan, aggrecan, and water. Chondrocytes are the only cells in cartilage and are responsible for maintaining and remodeling cartilage through a homeostatic balance of anabolic and catabolic activities. Under normal physiologic conditions, chondrocytes are exposed to millions of cycles of mechanical loading per year (1). These mechanical signals play an important role in regulating chondrocyte anabolic and biosynthetic activity, as evidenced by cartilage atrophy following periods of disuse or immobilization (2–7). However, under abnormal loading conditions (e.g., due to obesity, trauma, or joint instability), mechanical factors play a critical role in the onset and progression of osteoarthritis (1). Such "injurious" loading has been modeled in vitro using explant culture systems that replicate many of the early cellular and molecular events characteristic of osteoarthritis (8). Osteoarthritis is a painful and debilitating disease of weight-bearing joints that affects over 26 million people in the United States (9) with posttraumatic arthritis being responsible for ~12% of the incidence of osteoarthritis (10).

Despite the critical importance of mechanical loading in health and disease of synovial joints, the mechanisms of mechanotransduction of chondrocytes are not fully understood and are likely to differ under physiologic and pathologic conditions (11–14). Although many different mechanisms have been shown to be involved in chondrocyte mechanotransduction (13, 15–17), recent studies show that the cation channel, TRPV4, is responsible for mediating the anabolic response of chondrocytes to osmotic or mechanical stress (18–20). In this regard, identification of the mechanosensitive pathways involved in cartilage homeostasis as well as injury will help to provide novel targets for rational treatment of cartilage injury and posttraumatic osteoarthritis (21).

Recently, a new family of cation-permeable, directly mechanically activated (MA) ion channels, named "Piezo," has been identified in many cell types and several species including mammals (22, 23). These channels are Ca^{2+} permeable and can rapidly inactivate following mechanical gating. Piezo1 plays an important role in mechanotransduction in red blood cells and bladder urothelium, and mutations have been linked to human anemia and xerocytosis (24–28). Piezo2 is important for touch sensation in mammals and may play a role in somatosensory mechanotransduction of noxious stimuli (22, 29–31). However, the presence and function of Piezos in musculoskeletal tissues, which are exposed to a wide range of mechanical stimuli, have not been investigated.

In this study, we examined the expression and function of Piezos in cartilage and primary chondrocytes, as well as the synergistic action of Piezo1 and -2 in transducing mechanical signals

Significance

Cartilage, a mechanically sensitive tissue that covers joints, is essential for vertebrate locomotion by sustaining skeletal mobility. Transduction of mechanical stimuli by cartilage cells, chondrocytes, leads to biochemical–metabolic responses. Such mechanotransduction can be beneficial for tissue maintenance when evoked by low-level mechanical stimuli, or can have health-adverse effects via cartilage-damaging high-strain mechanical stress. Thus, high-strain mechanotransduction by cartilage mechanotrauma is relevant for the pathogenesis of osteoarthritis. Molecular mechanisms of high-strain mechanotransduction of chondrocytes have been elusive. Here we identify Piezo1 and Piezo2 mechanosensitive ion channels in chondrocytes as transduction channels for high-strain mechanical stress. We verify their functional link to the cytoskeleton as important for their concerted function and offer a remedial strategy by application of a Piezo1/2 blocking peptide, GsMTx4, from tarantula venom.

Author contributions: W.L., F.G., and W.B.L. designed research; W.L., H.A.L., Y.C., S.H.L., N.A.Z., A.L.M., J.W., K.N.B., and F.S. performed research; W.L., H.A.L., N.A.Z., J.W., K.N.B., J.C., S.Z., J.G., F.S., F.G., and W.B.L. contributed new reagents/analytic tools; W.L., H.A.L., J.W., A.L.M., F.S., F.G., and W.B.L. analyzed data; and W.L., H.A.L., A.L.M., F.G., and W.B.L. wrote the paper.

The authors declare no conflict of interest.

This article is a PNAS Direct Submission.

Freely available online through the PNAS open access option.

[1]To whom correspondence may be addressed. Email: wolfgang@neuro.duke.edu or guilak@duke.edu.

This article contains supporting information online at www.pnas.org/lookup/suppl/doi:10.1073/pnas.1414298111/-/DCSupplemental.

in a model cell line. Furthermore, we examined the role of Piezos in mechanically induced cell death in a cartilage tissue explant model. We report here that Piezo1 and -2 are functionally expressed in mammalian chondrocytes; high strain leads to Ca^{2+} influx into chondrocytes via PIEZO channels; and inhibiting Piezos with the peptide GsMTx4 protects articular chondrocytes from mechanically induced cell death.

Results

Robust Expression of Piezo Channels in Primary Chondrocytes. To examine whether Piezo channels are expressed in mammalian articular cartilage, we measured their presence and quantity in articular cartilage relative to other tissues in the mouse. Using Piezo-specific primers, we conducted real-time quantitative PCR (RT-qPCR) of mouse organs including bladder, lung, skin, trigeminal ganglion (TG), and articular cartilage (prepared from hip and knee joints). All mRNA levels were normalized to that of lung (Fig. 1 *A* and *B*). Both Piezo1 and Piezo2 (Piezo1/2) were robustly expressed in chondrocytes. Piezo1 mRNA levels in chondrocytes were higher than bladder, TG, and skin, and similar to lung. Piezo2 was expressed in cartilage at a similar level as bladder and skin, not reaching the levels of lung and TG. We then confirmed appreciable Piezo1/2 expression at the mRNA level in both porcine and human primary chondrocytes by RT-qPCR (Fig. 1 *C* and *D*). In porcine articular cartilage, we also detected Piezo1/2 by immunostaining (Fig. 1*E*), also in isolated chondrocytes (Fig. S1). The

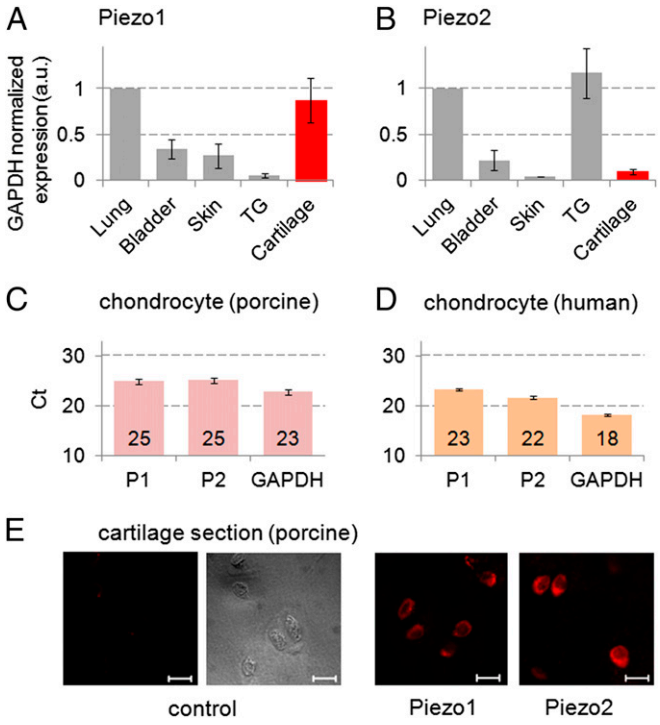

Fig. 1. Piezo1 (P1) and Piezo2 (P2) are robustly expressed in chondrocytes. (*A* and *B*) mRNA expression was measured by real-time quantitative PCR (RT-qPCR) using the $\Delta\Delta C_t$ method for analysis of relative gene expression levels in bladder, lung, skin, trigeminal ganglion (TG), and joint cartilage (hip, knee) of 4-wk-old male mice. Organs (except cartilage) were sampled from single mice (n = 6–10) and mRNA abundance was averaged. Cartilage was pooled (n = 3 pools from three, three, and four mice) to generate sufficient amounts of starting material. Glyceraldehyde-3-phosphate dehydrogenase (GAPDH) was used as a housekeeping gene for normalization, and expression in lung was assigned a numerical value of "1." (*C*) RT-qPCR Ct values of Piezo1, Piezo2, and GAPDH, based on RNA isolated from (*C*) porcine chondrocytes (n = 6 pigs) and (*D*) human chondrocytes (n = 4 subjects). (*E*) Piezo1- and Piezo2-specific immunolabeling of chondrocytes in porcine cartilage tissue. (Scale bar, 10 μm.)

appreciable expression of Piezo1/2 in isolated primary chondrocytes as well as in situ in cartilage raises the question of whether PIEZO channels function as physiologically relevant mechanotransducers. In this respect, it is worth bearing in mind that mRNA and protein expression is not the same as functional protein expression, especially for mechanosensitive channels where mechanical stress affecting the channels may be highly dependent on factors such as shielding of the channels from stress (32).

To verify functional expression of Piezo1/2 in chondrocytes, we tested their mechanosensitivity while inhibiting PIEZO signaling or knocking down Piezo1 or -2. In addition we modeled chondrocytes' Piezo1/2 coexpression in a permanent cell line with heterologous expression of Piezos, which allowed us to measure Ca^{2+} transients and transmembrane currents in response to mechanical stimulation.

MA Ca^{2+} Influx in Neuro2A Cells Overexpressing both Piezo1 and Piezo2. Because both Piezo1 and Piezo2 were expressed in articular chondrocytes, we first modeled the potential interaction of this dual expression in heterologously transfected cells. This approach allowed us to take full conceptual advantage of heterologous transfection of mechanosensitive Piezo channels in a cell line with minimal intrinsic response. This approach will clearly identify whether cotransfected Piezo1/2 shows a different response from singly transfected Piezo. To assess the mechanosensitivity of individual cells to controlled loading, we measured Ca^{2+} transients in individual cells using a custom-built atomic force microscope (AFM) Ca^{2+}-imaging setup. The mechanical stimulus that we used was AFM-driven compression with a force of up to ∼500 nN, applied via a tipless cantilever to smoothly compress a large region of the cell while minimizing local trauma (Fig. 2*A* and Movie S1). We used neuro2A (N2A) cells for this purpose because under our control conditions, they had no response to mechanical stimulation at the levels of strain we used. This finding is in contrast to the use of N2A cells to initially isolate Piezo channels (22) and emphasizes that one cannot rely upon specific lines of cells assuming they have consistent properties. N2A cells firmly adhere to the culture dish and do not robustly express functional Piezos (Fig. 2*B* and Fig. S1). We examined mechanical responses measured by Ca^{2+} influx after directed expression of Piezo1, Piezo2, and their coexpression. Piezo2-transfected cells showed no response to loading, and Piezo1-transfected cells showed a minimal response. In striking contrast, in Piezo1/2 cotransfected cells, AFM compression caused a robust and sustained Ca^{2+} influx with a peak Ca^{2+} increase of 588 ± 170 nM and a transient duration of 22 ± 6 s. The Ca^{2+} transients of Piezo1 or Piezo2 singly expressed were reduced to <10% (ΔCa^{2+} ≤52 nM) (Fig. 2 *B*–*F*). The stiffness of N2A cells was similar to that of chondrocytes, suggesting they have similar mechanical properties (Fig. S2). In keeping with this finding, we also noted the resemblance of the actin cytoskeleton in N2A cells with directed coexpression of PIEZO1/2 to the actin cytoskeleton of chondrocytes (Fig. S3).

MA Currents in N2A Cells Overexpressing both Piezo1 and Piezo2. With patch-clamp electrophysiology in cell-attached mode using N2A cells, we recorded the response to negative pressure steps that stretched the patch (22, 33). Patches of control cells did not produce current in response to suction. We confirmed and extended the results of our AFM Ca^{2+} imaging with whole-cell recordings. The currents revealed synergistic effects caused by coexpression of Piezo1 and Piezo2, versus expression of either transgene alone. We observed twofold higher peak currents (I_{max} ∼145 ± 26 pA) when channels were cotransfected than with a single-type transfection. The increase in plateau current was even more striking in cotransfected cells, $I_{plateau}$ ∼75 ± 10 pA, a sixfold increase over Piezo1-transfected cells (Fig. 2 *H*–*M*). Surprisingly, but consistent with our AFM data, suction did not

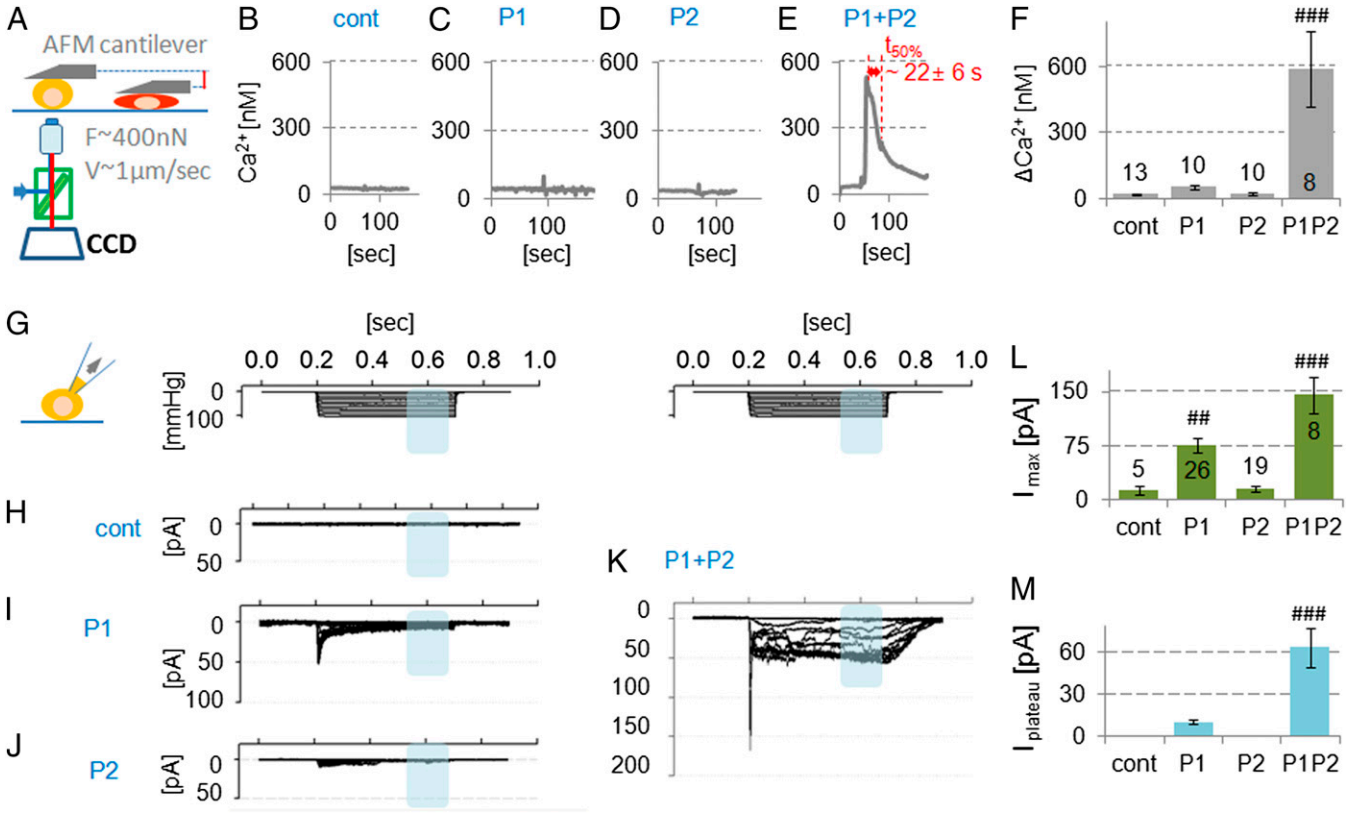

Fig. 2. Directed coexpression of Piezo1 and Piezo2 potentiates mechanically induced Ca^{2+} signals and transmembrane currents. (*A*) N2A transfected cells were mechanically stimulated by compressive mechanical loading (~400 nN, using a flat AFM probe) while recording intracellular Ca^{2+}. N2A cells with directed expression of (*B*) GFP, (*C*) Piezo1, (*D*) Piezo2, and (*E*) Piezo1 and Piezo2. Stimulated N2A cells overexpressing Piezo1 or Piezo2 (*B* and *C*) show rapidly decaying modest spikes (~30 nM Ca^{2+} influx). Note in contrast the robust Ca^{2+} signal (~500 nM) in N2A cells expressing both Piezo1 and Pieo2 (*E*). (*F*) Maximal $[Ca^{2+}]i$, prestimulation subtracted (ΔCa^{2+}). (*G*) Stepwise negative pressure induced transmembrane electrical currents in cell-attached mode: negative pipette pressure 0 to −100 mmHg, Δ−10 mmHg for 500 ms, holding potential of −65 mV. N2A cells were directed to express (*H*) nontransfected, (*I*) Piezo1, (*J*) Piezo2, and (*K*) Piezo1 and Piezo2. (*L*) Maximum amplitude of membrane stretch-evoked current is shown. (*M*) Maximum average plateau currents between ~350 and 450 ms are shown (blue shades in *K*). For *L* and *M*, note the potentiation of the signal for coexpression of PIEZO1 and PIEZO2. Bars represent the mean ± SEM; the number of cells tested (*n*) is shown in the bars in *F* and *L*. Significantly different from all other bars: $^{\#\#}P < 0.005$, $^{\#\#\#}P < 0.0005$, ANOVA, LSD post hoc.

evoke a significant current in patches from Piezo2-transfected cells. AFM Ca^{2+} and electrophysiology measurements suggested that PIEZO1/2 coexpression leads to increased sensitivity to mechanical stimulation. Importantly, two different types of mechanical cues, namely compression and suction-evoked membrane stretch, could activate PIEZO1/2.

See *SI Results* for kinetic modeling of PIEZO1/2 coexpression in N2A cells, an analysis which confirms and extends our conclusion of a synergistic function of PIEZO1 and PIEZO2 (Fig. S4).

MA Ca^{2+} Influx in Primary Chondrocytes. We then examined the mechanically activated Ca^{2+} signaling in primary porcine chondrocytes that natively express Piezo1/2 (Fig. 1*C*). We characterized the force-strain Ca^{2+}-influx relationship by compressing chondrocytes by 10, 50, 100, 300, and 500 nN, which resulted in nominal strains of ~12%, 25%, 45%, 50%, and 60% of cell height, respectively, resembling our results in N2A cells (Fig. S2 and Fig. 3 *A*–*C*).

At these forces, chondrocytes deformed significantly. This striking cellular behavior is shown in Fig. 3*C* and Movie S2. After compression, chondrocytes rapidly recovered their spherical shape and retained the fluorescent Ca^{2+} dye after lifting the AFM cantilever. These responses suggest that the cell membrane was not damaged and the cells displayed no plastic deformation. Chondrocyte Ca^{2+} levels increased significantly at forces >300 nN (Fig. S5). The resulting 50% strain is considered hyperphysiologic and injurious (3, 34–36). The Ca^{2+} transients (Fig. 3*B*) resembled those seen in heterologous cells with cotransfection of PIEZO1/2. They are not only robust in terms of amplitude, but also significantly longer lasting than those typically seen in PIEZO1- or PIEZO2-expressing N2A cells.

For attempts to obtain electrophysiology from mechanically stimulated chondrocytes, see *SI Results*.

siRNA-Mediated Piezo Knockdown Attenuates Ca^{2+} Transients in Primary Chondrocytes. We used siRNA to estimate the contributions of Piezo1 and Piezo2 to mechanically activated Ca^{2+} signaling in chondrocytes. We knocked down each Piezo and demonstrated the >50% efficiency of the respective knockdown by RT-qPCR (Fig. 3 *D*–*G*). We then subjected the siRNA-treated chondrocytes (single siRNA) to mechanical stimulation and observed a robust attenuation of the AFM Ca^{2+} transients, a similar effect for each knockdown. These results confirm the core concept of our study that both Piezos cooperatively participate in chondrocyte mechanotransduction at high strains. We note that our conclusion is based on incomplete knockdown of Piezo expression, so that simple attenuation of Piezo expression leads to attenuation of mechanical sensitivity to injurious strain.

Contributors to the High Mechanically Activated Ca^{2+} Influx in Primary Chondrocytes. To address the participation of PIEZO1/2 in a mechanotransduction complex, we characterized the AFM Ca^{2+} response of primary chondrocytes in more detail. We first

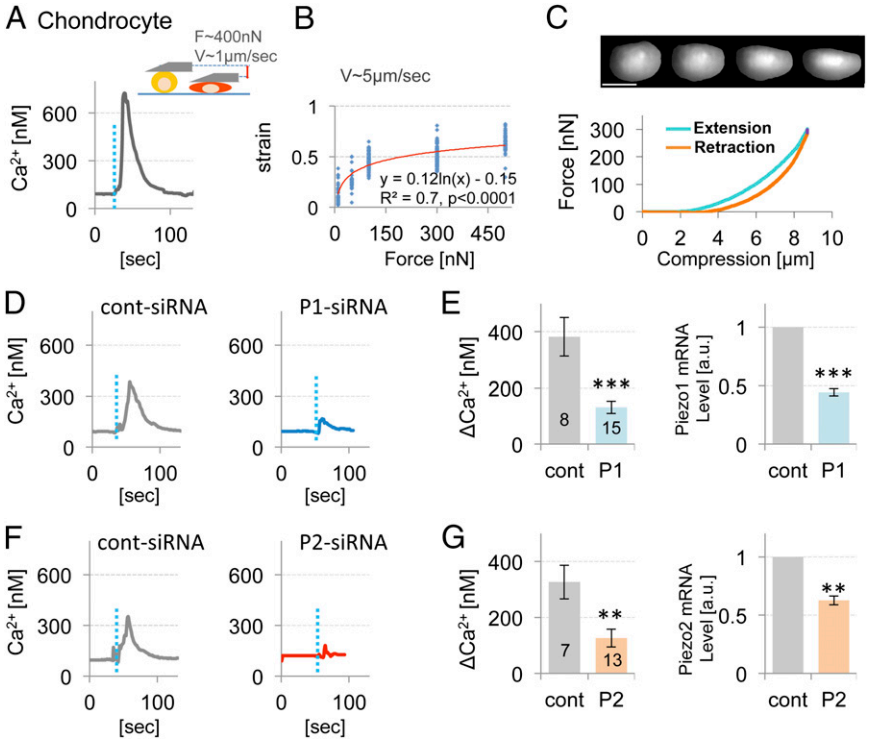

Fig. 3. High-strain AFM indentation induced Ca^{2+} influx and its suppression by Piezo knockdown suggest Piezo-mediated mechanotransduction in articular chondrocytes. (*A*) Schematic diagram of AFM indentation and a representative trace of mechanically activated Ca^{2+} influx of control chondrocytes ($F = 400$ nN, 1 μm/s ramp speed, dotted blue line indicates compression). (*B*) Cell strain increased significantly with applied force over a range of 10–500 nN (logarithmic regression of strain vs. ln(force), $P < 0.0001$). (*C*, *Upper*) Sequential images of the side view of a chondrocyte being compressed with an AFM cantilever, showing a smooth lateral expansion as the cell is compressed vertically. (Scale bar, 5 μm.) (*Lower*) Force curve from the same cell, showing force increase dependent on compression (*x* axis showing compression in micrometers). Note that we could not exert more than 300 nN force when using the AFM-PRISM microscope setup. (*D*) AFM-mediated Ca^{2+} influx of chondrocytes transfected with control siRNA (*Left*) and with Piezo1-targeting siRNA (*Right*) (50 nM siRNA each). (*E*) The average maximal Ca^{2+} influx and the mRNA level of Piezo1 determined by RT-qPCR. (*F*) AFM-mediated Ca^{2+} influx curves of chondrocytes transfected with control siRNA (*Left*) and with Piezo2-targeting siRNA (*Right*) (15 nM siRNA each); the average maximal Ca^{2+} influx and the mRNA expression level of Piezo2 are shown in *G*. Note robust attenuation of mechanically activated Ca^{2+} influx of chondrocytes subjected to Piezo1 or Piezo2 knockdown. GAPDH was used for normalization, $\Delta\Delta C_t$ method. Bars represent the mean ± SEM; the number of cells tested (*n*) is shown in bars. $^{**}P < 0.005$, $^{***}P < 0.0005$, unpaired *t* test.

verified the source of Ca^{2+} as extracellular, rather than from intracellular stores. Reducing extracellular Ca^{2+} greatly diminished the Ca^{2+} response, whereas depletion of intracellular stores with thapsigargin did not alter the response (Fig. 4 *A*–*C*). Second, we tested the involvement of the chondrocyte actin cytoskeleton in mechanotransduction because it is known to modulate mechanical sensitivity (37–39). Cytochalasin-D, a potent inhibitor of actin polymerization, led to a strong reduction of the Ca^{2+} signal (Fig. 4*D*). We next used ruthenium red (RR), which exhibits known PIEZO-channel blocking properties (22). RR inhibited the Ca^{2+} influx transients (Fig. 4*E*). Taken together, the reduction of extracellular of Ca^{2+} and the application of RR led to virtual elimination of the Ca^{2+} signal. These findings are consistent with the AFM Ca^{2+} response being mediated by PIEZO channels as suggested by our siRNA knockdown experiments. Their dependence on the actin cytoskeleton and extracellular Ca^{2+}, not intracellular stores, is an important new feature of PIEZO1/2 channels in articular chondrocytes. Critical involvement of the actin cytoskeleton also raises the question of other cytoskeletal elements and mechanisms playing an important role in this mechanotransduction process, e.g., dynamin related (see below).

Next, we tested the specific PIEZO inhibitor peptide, GsMTx4 (40, 41). In Piezo1/2 cotransfected N2A cells, we observed that 40 μM of GsMTx4 inhibited the AFM Ca^{2+} response almost completely (Fig. S6). In articular chondrocytes, GsMTx4 reduced the Ca^{2+} response in a dose-dependent manner with 40 μM being equipotent to external Ca^{2+} removal or RR block (Fig. 4*I*). The effect of GsMTx4 was fully reversible after wash-off (Fig. S7). At 20 μM, GsMTx4 increased the inactivation time and reduced the amplitude of the AFM Ca^{2+} transient (Fig. 4 *H* and *K*). At 2 μM, it had no effect on the Ca^{2+} transients ($\Delta Ca^{2+} = 369$ nM for control vs. 405 nM for 2 μM GsMTx4, $n = 4$, $P = 0.7$, unpaired *t* test). At 20 μM GsMTx4, the reduced amplitude is in keeping with the known PIEZO-inhibitory activity of the peptide. The observed appreciable increase of the inactivation time with 20 μM GsMTx4, against expectation because GsMTx4 acts primarily on the open state (42), is yet another unique property of PIEZO1/2 coexpression in chondrocytes.

As mechanotransductory channels, PIEZO channels form a close functional unit with the plasma membrane (43–45), also demonstrated by the inhibitory effect of GsMTx4, which acts as a gating modifier that inserts at the channel–lipid interface (32). Against this background, we decided to next test the function of dynamin, recently referred to as "membrane remodeler" (46), on PIEZO mechanotransductory function in chondrocytes. For this purpose, we inhibited dynamin GTPase with the selective inhibitor, dynasore (47). Dynasore (5 μM) led to a moderate (~65%) attenuation of the AFM Ca^{2+} signal, comparable to the one evoked at 100 nN compressive force (Fig. 4*G* and Fig. S5). This finding indicates that dynamin, presumably dynamin-2 in chondrocytes (46), affects mechanotransduction by PIEZO channels. To explore underlying cellular signaling correlates of this finding, we studied PIEZO1/2 coexpressing N2A cells. We identified an effect of dynamin inhibition on Piezo cellular

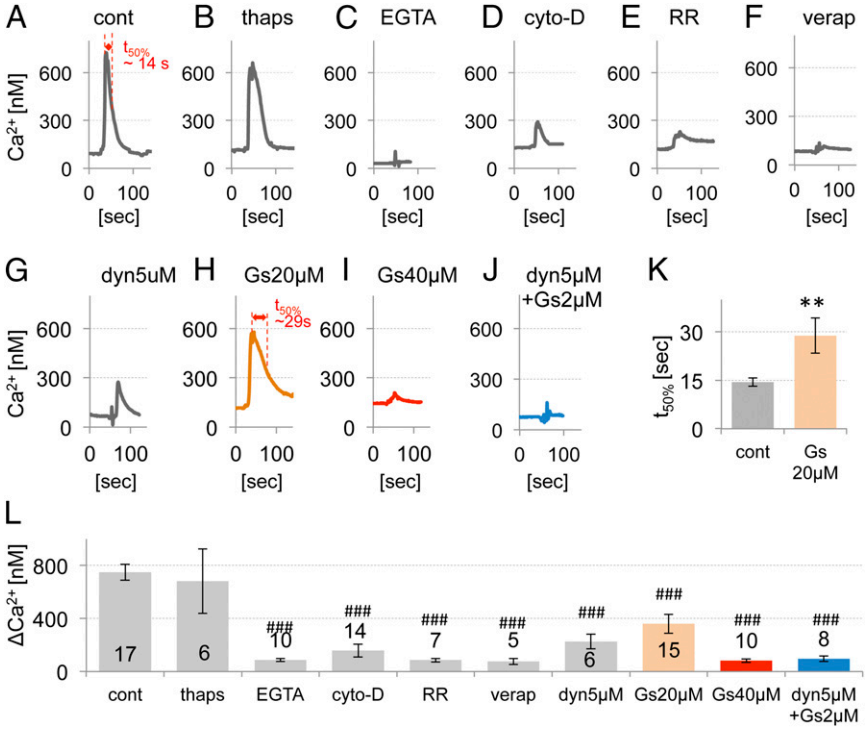

Fig. 4. Characteristics of mechanically evoked Ca^{2+} transients in primary chondrocytes. (*A–J*) Representative traces of mechanically activated Ca^{2+} influx of chondrocytes (400 nN force, 1 μm/s ramp speed), specifically treated with (*A*) vehicle-control (cont), (*B*) thapsigargin (thaps) 1 μM, (*C*) EGTA 10 mM, (*D*) cytochalasin-D (cyto-D) 2 μM, (*E*) ruthenium red (RR) 1 μM, (*F*) verapamil ~0.1–0.5 μM, (*G*) dynasore (dyn) 5 μM, (*H*) GsMTx4 (Gs) 20 μM, (*I*) GsMTx4 40 μM, and (*J*) GsMTx4 2 μM and dynasore 5 μM. (*K*) Average inactivation time ($t_{50\%}$) of control (shown in *A*) and GsMTx4 20 μM (shown in *H*). $^{**}P < 0.005$, unpaired *t* test. (*L*) Average maximum $[Ca^{2+}]i$ (ΔCa^{2+}, prestimulation subtracted). Bars represent the mean ± SEM; the number of cells tested (*n*) is shown in the bars. Significantly different from control, not different from each other (ANOVA, $^{\#\#\#}P < 0.0005$, Dunnett's post hoc).

trafficking, namely that cytoplasmic Piezo retention was decreased in dynasore-treated cells (Fig. 5 and Fig. S8). This finding suggests that Piezo channels might have increased outer plasma membrane expression caused by inhibition of dynamin GTPase. This phenomenon renders PIEZO channels more likely to become inactivated, providing a possible explanation for dynasore's effect. Based on our N2A–Piezo1/2 model, we reason that a moderate role can be attributed to how dynamin influences mechanical activation of PIEZO1/2 in chondrocytes. Because GsMTx4 was only fully effective at increased concentrations, we thus arrived at the critical question of whether inhibition of dynamin GTPase would boost the inhibitory potency of GsMTx4. Interestingly, we found that the effect of GsMTx4 was potentiated by 5 μM dynasore so that GsMTx4 only required 2 μM to inhibit the channels, an ineffective concentration by itself. Dynasore reduced the effective K_D of GsMTx4 to 20-fold lower than that without dynasore. See *Discussion* for a more in-depth discourse on these findings. See *SI Results* for negative results of a control experiment using chlorpromazine, an amphipathic compound devoid of effects on dynamin, and lacking a classical signaling target in chondrocytes (Fig. S9). Also in *SI Results* find evidence for lack of inhibition of hypotonically activated TRPV4 by GsMTx4 (18) (Fig. S10).

We also tested the role of L-type voltage-gated Ca^{2+} channels, which are known to be expressed in articular chondrocytes (48). We asked whether these channels could possibly be contributory to the Ca^{2+} signal via a downstream amplification mechanism after mechanical activation of PIEZOs, which would depolarize the cell. In keeping with this reasoning, inhibition with verapamil attenuated the Ca^{2+} transient in response to AFM-mediated compression (Fig. 4*F*). The critical contribution of L-type voltage-gated Ca^{2+} channels (VGCCs) to the Ca^{2+} response of articular chondrocytes to injurious strain sets this signaling mechanism apart from hypotonic cell swelling-evoked Ca^{2+} transients, which involve TRPV4 and do not rely on L-type voltage-gated Ca^{2+} channels (18, 49).

GsMTx4 Significantly Protects Mechanically Injured Articular Cartilage. Because our results in primary cells suggested a cellular response to an injurious stimulus, we tested the response in articular chondrocytes in a cartilage explant model system. We assessed the effect of PIEZO inhibition in a cartilage injury model where osteochondral explants were subjected to mechanical injury with a biopsy punch device, resulting in high local strains that damage the chondrocytes around the cut edge. The resulting damage area, the "zone of death," surrounding the wound was assessed quantitatively using a fluorescent live/dead assay. We tested whether GsMTx4 might protect chondrocytes from cell death following injury. Preincubation with GsMTx4 (40 μM) significantly decreased the zone of death surrounding the wound (Fig. 6). These findings show that a Piezo1/2-mediated mechanotransduction pathway modulates chondrocyte injury, and blocking this pathway is protective. GsMTx4 is commercially available and nontoxic (50, 51) making it a potentially useful therapeutic agent for targeting Piezo1/2 so that progressive cartilage degeneration following joint trauma can hopefully be addressed more rationally.

Discussion

Our studies show that Piezo1 and Piezo2 are expressed in articular chondrocytes. Although physiologic levels of cell deformation did not appear to activate these channels, they did respond to hyperphysiologic strains. GsMTx4, a biologically derived peptide that specifically inhibits mechanically activated cation channels, and that we demonstrate here to inhibit heterologously coexpressed

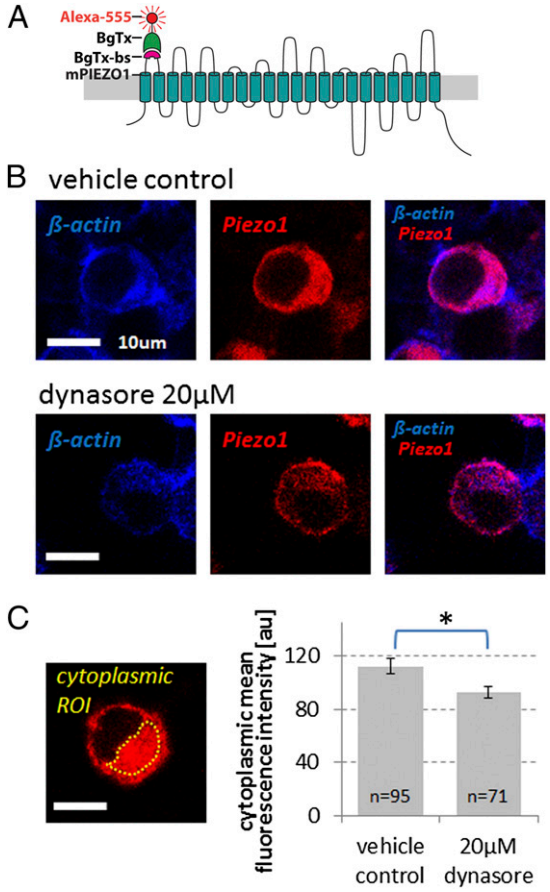

Fig. 5. Surface-labeled Piezo1 channels are less abundant in the cytoplasm in response to inhibition of dynamin GTPase in Piezo1/2 cotransfected N2A cells. (*A*) Schematic representation of bungarotoxin binding site (BgTx-bs) engineered into the first extracellular loop of mPiezo1 labeled with bungarotoxin (BgTx), conjugated to Alexa Fluor 555. These channels are fully functional (Fig. S8). (*B*) Representative confocal micrographs of N2A cells transfected with Piezo1-BgTx-bs (see *A*), exposed in vivo to BgTx-Alexa-555 (red) for 15 min, and labeled postfixation with phalloidin-CF350 (blue). *Top Row* shows a vehicle control-treated cell; *Bottom Row*, a cell treated with dynamin GTPase inhibitor dynasore (20 μM); cells were treated for 3 h. (Scale bar, 10 μm.) (*C*) Exemplary cytoplasmic ROI (confined by the yellow dotted line, note nuclear sparing). Bar diagram shows relative comparison of the mean fluorescence intensity of cytoplasmic BgTx labeling, background subtracted. Averaged *n* of quantified cells is given in the bars, which indicate mean ± SEM (error bars); $*P = 0.014$, unpaired *t* test.

Piezo1/2, attenuated the response of chondrocytes to injurious mechanical strain. GsMTx4 also showed potential as a chondroprotective agent in our cartilage explant model system. Our results establish the novel concept that articular chondrocytes, which are physiologically nonneural mechanosensitive cells, functionally express both Piezo channels with apparent synergy that contributes to mechanosensitivity.

Chondrocytes are exposed to a variety of physical and mechanical stimuli during physiologic and pathologic joint loading, and thus the ability to perceive and respond properly to these signals is critical for the maintenance of joint health (1). Our discovery provides, to our knowledge, the first direct evidence that mechanically sensitive ion channels in articular chondrocytes are necessary for these cells' response to high-strain mechanical cues. These findings complement recent results from our group reporting that the anabolic response of chondrocytes to low-level, physiologic mechanical loading, is regulated by a TRPV4-based mechanism (20). In addition, we have previously reported that loss of TRPV4 leads to age-dependent osteoarthritis in mice (19).

The current findings are consistent with previous studies suggesting the high sensitivity of chondrocytes to osmotic stress (14, 52), but decreased sensitivity to low-level mechanical strains induced by cell indentation or micropipette aspiration (53, 54). There appear to be multiple, functionally specific mechanisms of mechanical signal transduction in this nonneural cell type. Functional expression of TRPV4 and PIEZO1/2 (and potentially other channels) (55, 56) in articular chondrocytes allow cells to respond to the continuum of mechanical loads in cartilage. The findings of this study, together with those in the literature, suggest that chondrocyte mechanosensation involves an integrated set of pathways that may also include transmission of pericellular mechanical and osmotic signals to the cell and nucleus via integrins and various cytoskeletal components (17, 57–61).

Understanding the relevant mechanisms—biophysical, molecular, protein–protein, physiological, signaling—of PIEZO channel function in chondrocytes is a rational path toward understanding cartilage mechanobiology and associated diseases, particularly osteoarthritis (21). Several important questions remain for follow-up studies. How does the PIEZO1/2 synergism function at the molecular level? Do PIEZO1 and PIEZO2 form heteromeric channels? Do articular chondrocytes express homomeric channels that are activated sequentially, or simultaneously, or does the dual expression lead to changes in the cytoskeleton that alter the stress in the channels? As we show here, Ca^{2+} influx in response to injurious mechanical strain can be affected by L-type voltage-gated Ca^{2+} channels, suggesting an important signaling link. This signal transduction chain is in keeping with a recent publication (48) that reports a key role for L-type voltage-gated channels in osteoarthritis, evoked and aggravated by mechanical trauma. We consider it an appealing possibility that the chondrocytic Ca^{2+} signal of cartilage traumatic injury impacts chondrocytes' cytoskeleton, energy homeostasis, apoptotic equilibrium, and inflammatory phenotype (15, 62–65).

Another important result of our experiments was that an ineffective low dose of GsMTx4 was rendered highly potent—with a 20-fold increase in potency—by coapplication of an otherwise mildly effective dose of dynasore, a dynamin GTPase inhibitor. It is likely that dynasore exerted its GsMTx4-potentiating effect by inhibiting GTPase activity of dynamin-2 in chondrocytes, the main dynamin in these cells (46). For interaction with outer plasma membrane mechanotransducer ion channels, other dynamin-like proteins are not very suitable targets (46, 47). We believe that the most striking aspect of dynasore's action—potentiation of low-dose GsMTx4—are rooted in the known effect of dynamin on membrane curvature (66, 67). Dynamin, also referred to as mechanochemical GTPase (68), according to this interpretation, could contribute to lack of effect at lower doses of GsMTx4, by its link to membrane curvature so that GsMTx4 peptide could not insert itself in a very efficient way at the channel–lipid interface to inhibit PIEZO1/2 in chondrocytes. As a result, as observed, PIEZO1/2 channels in chondrocytes are not particularly responsive to GsMTx4. Dynasore inhibition of dynamin GTPase would reduce this regulatory function of dynamin so that GsMTx4 becomes significantly more potent, as observed in our experiments. An alternate, not mutually exclusive possibility can also be considered. If PIEZO channels can be endocytosed, and if they are inhibited by dynasore from leaving the plasma membrane, they may become a more ready target for GsMTx4. This could be a complementary mechanism, in addition to dynamin's effect on membrane curvature. However, the main shortcoming of this concept is that dynasore alone attenuated, not potentiated, the effect of AFM-mediated compression of chondrocytes. With a postulated critical effect of inhibition of PIEZO1/2 endocytosis, the channel should be present more abundantly in the plasma membrane, prima vista increasing mechanotransduction Ca^{2+} transients, not decreasing them.

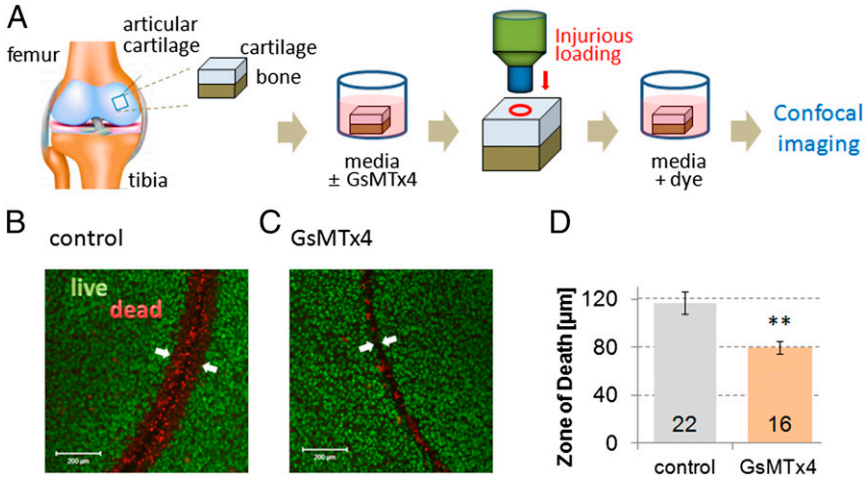

Fig. 6. GsMTx4-mediated PIEZO inhibition is chondroprotective in a cartilage explant injury model. (*A*) Our explant model in a schematic. (*B* and *C*) Live/dead (green/red) staining shows a zone of death around biopsy wound edge in representative control and 40 μM GsMTx4-treated samples. (Scale bar, 200 μm.) (*D*) Mean zone of death is significantly decreased in cartilage treated with GsMTx4. Bars represent the mean ± SEM; numbers in bars represent experimental repeats. Significantly different from control $^{**}P < 0.005$, unpaired *t* test.

In aggregate, we favor the view that membrane remodeling by dynamin could have the effect of shielding PIEZO channels from the inhibitory effect of GsMTx4, at least valid for naturally expressed PIEZO1/2 in chondrocytes. Blocking dynamin's membrane remodeling effects with dynasore will then enhance the potency of GsMTx4, as observed in our experiments. There could be additional amphipathic effects of dynasore that facilitate its GsMTx4 potentiation, but another amphipathic molecule, chlorpromazine—devoid of effects on dynamin GTPase—had no effect on PIEZO inhibition by GsMTx4 in chondrocytes.

Chondrocyte death has been proposed as an important mechanism leading to posttraumatic arthritis following traumatic joint injury (36, 69, 70). PIEZO1/2, functionally expressed in joint cartilage, provide novel molecular targets for reducing cell death and mitigating injury-induced cartilage degeneration following joint trauma. Thus, targeting Piezos could potentially serve as a therapy for posttraumatic osteoarthritis. In this regard, GsMTx4 may be able to serve as a chondroprotective agent to prevent and treat osteoarthritis and other mechanically induced forms of the disease such as those caused by joint instability, misalignment, or obesity, by altering pathologic mechanical signal transduction pathways. Given the benign toxicity profile of GsMTx4, e.g., lack of cardiac effects (71, 72), future studies will examine this approach in animal models of joint injury, paving the way to human clinical trials.

Materials and Methods

Mouse Tissue RNA Extraction and RT-qPCR. Mouse organs were dissected from 4-wk-old male mice ($n = 10$). For cartilage, knee and hip cartilage ($n = 3$ samples; each sample contained pooled tissues from three to four mice) was harvested and stored in RNA-later (Life Technologies) until RNA extraction. Total RNA was extracted for subsequent RT-qPCR, as described previously (73–75). Glyceraldehyde-3-phosphate dehydrogenase (GAPDH) was used as a housekeeping gene for normalization, and expression in lung was defined as "1." All mouse experimentation was covered by a valid animal protocol of the Duke University Institutional Animal Care and Use Committee, abiding by all institutional, state, and federal (NIH) guidelines that govern use of animals in research.

Immunohistochemistry. A block of porcine articular cartilage tissue was fixed in paraformaldehyde and embedded in paraffin. Anti-Piezo1 rabbit antibody (Abcam) and anti-Piezo2 rabbit antibody (Novus) was applied to 12-μm sections and detected using a fluorescent secondary antibody (Alexa Fluor 555; Molecular Probes). Nonimmunized rabbit serum was used as negative control.

Chondrocyte Isolation and Culture. Chondrocytes were harvested from articular cartilage of the femoral condyles of skeletally mature (2–3 y old) female pigs (18, 76). The isolated chondrocytes were cultured on 12-mm round glass coverslips as described previously (18). Mechanical stimulation experiments were performed 2 d after cell isolation, and 3 d after isolation for siRNA transfections, which were performed on the day of isolation.

Chondrocyte AFM Compression and Ca^{2+} Imaging. The mechanotransduction events of single chondrocytes were measured using a custom-built AFM Ca^{2+} setup consisting of an AFM (Bioscope; Veeco) and a ratiometric Ca^{2+} imaging work station (Intracellular Imaging) (Fig. 2*A*). This setup is composed of an AFM head (contains *x-y-z* piezoelectric scanner and cantilever holder), AFM cantilever, sample stage with thermal equilibration (experiments conducted at 37 °C), inverted microscope (Intracellular Imaging) with 20×/0.8 NA Olympus objective for fluorescent microscopy, light source (340 nm, 380 nm dual wavelength stimulation), high-resolution CCD camera, and analysis software. Primary porcine chondrocytes or N2A cells were seeded on 12-mm diameter glass coverslips, then loaded with Ca^{2+} sensitive Fura-2-AM dye (2 μM for 30 min; Invitrogen) for ratiometric imaging (18, 77, 78). The piezoelectric scanner in the AFM head controls the *z* position of the AFM cantilever to compress individual cells. A cell of interest is compressed by the AFM cantilever to a prescribed force and then the cantilever is withdrawn. Meanwhile the ratiometric Ca^{2+} images are taken at wavelengths of 340 and 380 nm, and the transient Ca^{2+} concentrations, 340/380 ratio, are analyzed (InCytIm-2 software; Intracellular Imaging). Tipless cantilevers with spring constants of ~0.5–14 N/m (Novasan or Bruker Probes) were used. The compression rate was 1–2 μm/s. The force-displacement properties of individual cells were recorded to determine the nominal strain (% change in cell height) at each force level.

Neuro2A Cells with Directed Expression of Piezo1/Piezo2. N2A cells were examined using the AFM/Ca^{2+} setup. Neuro2A cells were transfected with mouse Piezo1 and/or Piezo2 plasmids (22) using Exgen500 (Fermentas). Piezo1-IRES-GFP plasmids were transfected for Piezo1 overexpression, whereas Piezo2 plasmids were cotransfected with eGFP plasmids, which were also used for control transfection, to identify transfected cells. For Piezo1/2 overexpression, no eGFP plasmid was used. All cDNAs were driven by CMV promoters. Transfected N2A cells, identified by fluorescence, were examined after 48 h. PCR analysis was conducted following ref. 77.

Chondrocyte siRNA Treatment. siRNAs targeting porcine Piezo1 and Piezo2 were designed, both of which specifically down-regulated their respective mRNA. The siRNAs and the control siRNA (nontargeting siRNA no. 1) were purchased from Dharmacon. siRNAs were transfected using electroporation with the SCN Nucleofector kit that employs the nucleofector device (Lonza). The designed Piezo1-targeting siRNA sequences are CAGCGAGAUCUCGCACUCCAUC, UACGACCUGCUGCAGCUCCUG, ACCCGCUGGCCAUGCAGUUCUU; the designed Piezo2-targeting siRNA sequences are CGACGAAGUCGAACAGUGAGUG and GAUCUGCGUGGAGGACAUUUAUG. To identify the transfected

cells, siRNA pools were cotransfected with an eGFP plasmid (provided with Lonza transfection kit), indicating a >80% transfection rate. Transfected cells were used 3 d posttransfection. Efficiency of siRNA was verified by RT-qPCR specific for the target using nontargeting control siRNA transfected cells as controls.

Piezo Expression Level in Chondrocytes by RT-qPCR. On the third day after the siRNA transfection, porcine (*Sus scrofa*) chondrocytes were lysed, total RNA was extracted, and the abundance of Piezo1 and Piezo2 transcripts was determined using established methods (73). For quantitation, we used the $2^{-\Delta\Delta CT}$ method (79). Primer sequences for ssPiezo1 were forward-GCCCCCAACGGACCTGAAGC and reverse-TGCGCAGCTGGATACGCACC and for ssPiezo2, forward-CCAGCTGGATCTGCGTGGAGG and reverse-TGGTTGATCACCCCGGCGAC. cDNA from human chondrocytes derived from normal control subjects (73) ($n = 4$) were also tested by RT-qPCR. Primer sequences for huPiezo1 were forward-CAATGAGGAGGCCGACTACC and reverse-GCACTCCTGCAGTTCGATGA and for huPiezo2, forward-GCCCAACAAAGCCAGTTGAA and reverse-GGGCTGATGGTCCACAAAGA.

Electrophysiology. We used a patch-clamp system similar to the one described previously (22, 80). Cells were placed on an inverted microscope (TI-S; Nikon) and currents were recorded with an EPC10 amplifier and Patchmaster software (HEKA) at a sampling rate of 5 kHz. Mechanical stimulation in the cell-attached configuration was performed by a pressure clamp system (ALAHSPC-1; ALA Scientific), where the negative pipette pressure was applied for 500 ms from 0 to −100 mmHg with −10 mmHg increments in 10-s intervals. The patch pipette solution and external bath solution contained (in millimolars) 150 NaCl, 3 KCl, 1 $MgCl_2$, 10 Hepes, 2.5 $CaCl_2$, 10 glucose, osmolarity adjusted to 320 mOsm with sucrose, and pH to 7.4. All experiments were done at room temperature.

Kinetics. The kinetic electrophysiology data from N2A patches were fit to state models of two or three states and independent channels, using the MAC and MERGE routines in QUB Express (www.qub.buffalo.edu).

Treatment with Compounds and GsMTx4. Chondrocytes were treated with ruthenium red (1 μM, 5 min; Tocris), cytochalasin-D (2 μM, 2 h; Tocris), thapsigargin (1 μM, 1 h; Sigma-Aldrich), EGTA (10 mM, 5 min), verapamil (0.1–0.5 μM, 20 min; Sigma-Aldrich), dynasore (5 and 20 μM, 2 h; Tocris), chlorpromazine (100 μg/mL, 1 h; Sigma-Aldrich), and D-enantiomer of GsMTx4 peptide (2, 20, and 40 μM, 5 min; provided by Philip Gottlieb, SUNY Buffalo) (81).

In Situ Piezo Function. Tissue explants of cartilage with underlying bone (~2 cm diameter) were removed from the femoral condyles of skeletally mature pigs. Explants were rinsed twice with PBS and transferred to media (phenol-red free DMEM, Hepes, L-glutamine, Na pyruvate, osmolarity adjusted to 300 mOsm with deionized water, pH 7.4). Explants were pretreated with 40 μM GsMTx4 for 2 h, 600 mOsm experimental media (osmolarity adjusted with sucrose) for 4 min (82), or control media before injury. Explants were injured by punching through the cartilage down to bone with a 3-mm stainless steel biopsy punch. Injured explants were incubated for 2 h postinjury in the same pretreatment solutions. Explants were then stained with the Live/Dead kit (calcein-AM stains live cells green, ethidium homodimer-1 stains dead cells red; Life Technologies). Four images were taken of the surface of each explant with a confocal microscope (LSM 510; Zeiss). The thickness of the zone of death, defined as the point at which half of the cells were viable, was measured using a custom-written code on each image (Matlab, The Mathworks).

Prism Microscopy. See *SI Results*.

Bungarotoxin Labeling of Piezo1. The 13-residue bungarotoxin (BTX) binding site (TGGAGATACTACGAGAGCTCCCTGGAGCCCTACCCTGAC) was cloned into the first extracellular loop of mouse Piezo1 predicted by the Phobius prediction program (www.ebi.ac.uk/Tools/pfa/phobius), using the Stratagene QuikChange Site-Directed Mutagenesis kit according to manufacturer protocol. The construct was transfected into N2A cells as described above. After dynasore treatment (2 h 45 min), cells were washed three times with 37 °C PBS and then incubated with α-bungarotoxin, Alexa Fluor 555 conjugate (Invitrogen) at a concentration of 10 μg/mL in PBS for 15 min at 37 °C. Cells were then washed again three times, 5 min per wash, with PBS and fixed and stained with 4% (wt/vol) paraformaldehyde, followed by permeabilization with 0.5% Triton-X, and labeled with phalloidin-CF350. Fluorescence of BTX-tagged receptors was determined in a cytoplasmic region of interest (ROI) using ImageJ freeware by measuring average signal density in the ROI and background subtraction, then averaging the signal for transfected cells subjected to dynasore treatment or vehicle control.

Functionality of BTX-Piezo1. The BTX-Piezo1 construct was transfected into HEK293T cells with Fugene6 (Promega) and recorded with patch clamp and pressure clamp systems as described above. The patch pipette solution contained (in millimolars) 130 NaCl, 5 KCl, 10 Hepes, 1 $CaCl_2$, 2 $MgCl_2$, and 10 TEA-Cl, pH to 7.3. The external bath solution contained (in millimolars) 140 KCl, 1 $MgCl_2$, 10 Hepes, and 10 glucose, pH to 7.3. The peak amplitude of each pressure step was normalized to the maximum response in the pressure step series and averaged across cells. The P50s were extracted from the Boltzmann fit of each individual cell and averaged.

Statistical Analysis. Average data are presented in a bar diagram as a mean ± SEM. Two-tail unpaired Student *t* test or one-way ANOVA and Fisher least significant difference (LSD) or Dunnett's post hoc test was used to determine the statistical significance. $*P \leq 0.05$, $**P \leq 0.005$, considered statistically significant.

ACKNOWLEDGMENTS. We thank Dr. Christopher Nicolai [State University of New York Buffalo (SUNY Buffalo)] for the kinetic analysis and Drs. Timothy O'Brien III, Richard Superfine, and Michael Falvo (Computer Integrated Systems for Microscopy and Manipulation, University of North Carolina at Chapel Hill) for help with AFM prism microscopy. Piezo1 and Piezo2 plasmids were kindly supplied by Dr. Ardem Patapoutian and GsMTx4 peptide by Dr. Philip Gottlieb (SUNY Buffalo). This work was supported in part by National Institutes of Health Grants AR048182, DE018549, DE01854952 (Administrative Supplement), R01HL054887, AG15768, AR50245, AR48852, AR065653, AG46927, and EB002025.

1. Guilak F (2011) Biomechanical factors in osteoarthritis. *Best Pract Res Clin Rheumatol* 25(6):815–823.
2. Grodzinsky AJ, Levenston ME, Jin M, Frank EH (2000) Cartilage tissue remodeling in response to mechanical forces. *Annu Rev Biomed Eng* 2:691–713.
3. Fitzgerald JB, et al. (2004) Mechanical compression of cartilage explants induces multiple time-dependent gene expression patterns and involves intracellular calcium and cyclic AMP. *J Biol Chem* 279(19):19502–19511.
4. Quinn TM, Grodzinsky AJ, Buschmann MD, Kim YJ, Hunziker EB (1998) Mechanical compression alters proteoglycan deposition and matrix deformation around individual cells in cartilage explants. *J Cell Sci* 111(Pt 5):573–583.
5. Ragan PM, et al. (1999) Down-regulation of chondrocyte aggrecan and type-II collagen gene expression correlates with increases in static compression magnitude and duration. *J Orthop Res* 17(6):836–842.
6. Valhmu WB, et al. (1998) Load-controlled compression of articular cartilage induces a transient stimulation of aggrecan gene expression. *Arch Biochem Biophys* 353(1):29–36.
7. Guilak F, Sah R, Setton LA (1997) Physical regulation of cartilage metabolism. *Basic Orthopaedic Biomechanics*, eds Mow VC, Hayes WC (Lippincott-Raven, Philadelphia), pp 179–207.
8. Stevens AL, Wishnok JS, White FM, Grodzinsky AJ, Tannenbaum SR (2009) Mechanical injury and cytokines cause loss of cartilage integrity and upregulate proteins associated with catabolism, immunity, inflammation, and repair. *Mol Cell Proteomics* 8(7):1475–1489.
9. Lawrence RC, et al.; National Arthritis Data Workgroup (2008) Estimates of the prevalence of arthritis and other rheumatic conditions in the United States. Part II. *Arthritis Rheum* 58(1):26–35.
10. Brown TD, Johnston RC, Saltzman CL, Marsh JL, Buckwalter JA (2006) Posttraumatic osteoarthritis: A first estimate of incidence, prevalence, and burden of disease. *J Orthop Trauma* 20(10):739–744.
11. Mobasheri A, et al. (2012) Potassium channels in articular chondrocytes. *Channels (Austin)* 6(6):416–425.
12. Wann AK, et al. (2012) Primary cilia mediate mechanotransduction through control of ATP-induced Ca2+ signaling in compressed chondrocytes. *FASEB J* 26(4):1663–1671.
13. Vincent TL, McLean CJ, Full LE, Peston D, Saklatvala J (2007) FGF-2 is bound to perlecan in the pericellular matrix of articular cartilage, where it acts as a chondrocyte mechanotransducer. *Osteoarthritis Cartilage* 15(7):752–763.
14. Chao PH, West AC, Hung CT (2006) Chondrocyte intracellular calcium, cytoskeletal organization, and gene expression responses to dynamic osmotic loading. *Am J Physiol Cell Physiol* 291(4):C718–C725.
15. Mobasheri A, Carter SD, Martín-Vasallo P, Shakibaei M (2002) Integrins and stretch activated ion channels; putative components of functional cell surface mechanoreceptors in articular chondrocytes. *Cell Biol Int* 26(1):1–18.
16. Kock LM, et al. (2009) RGD-dependent integrins are mechanotransducers in dynamically compressed tissue-engineered cartilage constructs. *J Biomech* 42(13):2177–2182.

17. Irianto J, et al. (2013) Osmotic challenge drives rapid and reversible chromatin condensation in chondrocytes. *Biophys J* 104(4):759–769.
18. Phan MN, et al. (2009) Functional characterization of TRPV4 as an osmotically sensitive ion channel in porcine articular chondrocytes. *Arthritis Rheum* 60(10):3028–3037.
19. Clark AL, Votta BJ, Kumar S, Liedtke W, Guilak F (2010) Chondroprotective role of the osmotically sensitive ion channel transient receptor potential vanilloid 4: Age- and sex-dependent progression of osteoarthritis in Trpv4-deficient mice. *Arthritis Rheum* 62(10):2973–2983.
20. O'Conor CJ, Leddy HA, Benefield HC, Liedtke WB, Guilak F (2014) TRPV4-mediated mechanotransduction regulates the metabolic response of chondrocytes to dynamic loading. *Proc Natl Acad Sci USA* 111(4):1316–1321.
21. Drexler S, Wann A, Vincent TL (2014) Are cellular mechanosensors potential therapeutic targets in osteoarthritis? *Int J Clin Rheumatol* 9(2):155–167.
22. Coste B, et al. (2010) Piezo1 and Piezo2 are essential components of distinct mechanically activated cation channels. *Science* 330(6000):55–60.
23. Xiao R, Xu XZ (2010) Mechanosensitive channels: In touch with Piezo. *Curr Biol* 20(21): R936–R938.
24. Zarychanski R, et al. (2012) Mutations in the mechanotransduction protein PIEZO1 are associated with hereditary xerocytosis. *Blood* 120(9):1908–1915.
25. Miyamoto T, et al. (2012) Piezo1, a novel mechanosensor in the bladder urothelium. *Neurourol Urodyn* 31(6):1015–1017.
26. Gottlieb PA, Bae C, Gnanasambandam R, Nicolai C, Sachs F (2013) Piezo1 mutations identified in xerocytosis alter the inactivation rate. *Biophys J* 104(2):467A–467A.
27. Demolombe S, Duprat F, Honoré E, Patel A (2013) Slower Piezo1 inactivation in dehydrated hereditary stomatocytosis (xerocytosis). *Biophys J* 105(4):833–834.
28. Andolfo I, et al. (2013) Multiple clinical forms of dehydrated hereditary stomatocytosis arise from mutations in PIEZO1. *Blood* 121(19):3925–3935, S1–S12.
29. Eijkelkamp N, et al. (2013) A role for Piezo2 in EPAC1-dependent mechanical allodynia. *Nat Commun* 4:1682.
30. Woo SH, et al. (2014) Piezo2 is required for Merkel-cell mechanotransduction. *Nature* 509(7502):622–626.
31. Maksimovic S, et al. (2014) Epidermal Merkel cells are mechanosensory cells that tune mammalian touch receptors. *Nature* 509(7502):617–621.
32. Gottlieb PA, Sachs F (2012) Piezo1: Properties of a cation selective mechanical channel. *Channels (Austin)* 6(4):214–219.
33. Guharay F, Sachs F (1984) Stretch-activated single ion channel currents in tissue-cultured embryonic chick skeletal muscle. *J Physiol* 352:685–701.
34. Choi JB, et al. (2007) Zonal changes in the three-dimensional morphology of the chondron under compression: The relationship among cellular, pericellular, and extracellular deformation in articular cartilage. *J Biomech* 40(12):2596–2603.
35. Li Y, et al. (2013) Moderate dynamic compression inhibits pro-catabolic response of cartilage to mechanical injury, tumor necrosis factor-alpha and interleukin-6, but accentuates degradation above a strain threshold. *Osteoarthritis Cartilage* 21(12): 1933–1941.
36. Stolberg-Stolberg JA, et al. (2013) Effects of cartilage impact with and without fracture on chondrocyte viability and the release of inflammatory markers. *J Orthop Res* 31(8):1283–1292.
37. Wang N, Butler JP, Ingber DE (1993) Mechanotransduction across the cell surface and through the cytoskeleton. *Science* 260(5111):1124–1127.
38. Balasubramanian L, Ahmed A, Lo C-M, Sham JSK, Yip K-P (2007) Integrin-mediated mechanotransduction in renal vascular smooth muscle cells: Activation of calcium sparks. *Am J Physiol Regul Integr Comp Physiol* 293(4):R1586–R1594.
39. Krieg M, Dunn AR, Goodman MB (2014) Mechanical control of the sense of touch by β-spectrin. *Nat Cell Biol* 16(3):224–233.
40. Bae C, Gnanasambandam R, Nicolai C, Sachs F, Gottlieb PA (2013) Xerocytosis is caused by mutations that alter the kinetics of the mechanosensitive channel PIEZO1. *Proc Natl Acad Sci USA* 110(12):E1162–E1168.
41. Bae C, Sachs F, Gottlieb PA (2011) The mechanosensitive ion channel Piezo1 is inhibited by the peptide GsMTx4. *Biochemistry* 50(29):6295–6300.
42. Gottlieb PA, Suchyna TM, Sachs F (2007) Properties and mechanism of the mechanosensitive ion channel inhibitor GsMTx4, a therapeutic peptide derived from tarantula venom. *Curr Top Membr* 59:81–109.
43. Martinac B (2004) Mechanosensitive ion channels: Molecules of mechanotransduction. *J Cell Sci* 117(Pt 12):2449–2460.
44. Coste B (2012) [Piezo proteins form a new class of mechanically activated ion channels]. *Med Sci (Paris)* 28(12):1056–1057.
45. Vásquez V, Krieg M, Lockhead D, Goodman MB (2014) Phospholipids that contain polyunsaturated fatty acids enhance neuronal cell mechanics and touch sensation. *Cell Reports* 6(1):70–80.
46. Ferguson SM, De Camilli P (2012) Dynamin, a membrane-remodelling GTPase. *Nat Rev Mol Cell Biol* 13(2):75–88.
47. Macia E, et al. (2006) Dynasore, a cell-permeable inhibitor of dynamin. *Dev Cell* 10(6): 839–850.
48. Takamatsu A, et al. (2014) Verapamil protects against cartilage degradation in osteoarthritis by inhibiting Wnt/β-catenin signaling. *PLoS ONE* 9(3):e92699.
49. Sánchez JC, Danks TA, Wilkins RJ (2003) Mechanisms involved in the increase in intracellular calcium following hypotonic shock in bovine articular chondrocytes. *Gen Physiol Biophys* 22(4):487–500.
50. Suchyna TM, Sachs F (2007) Mechanosensitive channel properties and membrane mechanics in mouse dystrophic myotubes. *J Physiol* 581(Pt 1):369–387.
51. Yeung EW, et al. (2005) Effects of stretch-activated channel blockers on [Ca2+]i and muscle damage in the mdx mouse. *J Physiol* 562(Pt 2):367–380.
52. Erickson GR, Alexopoulos LG, Guilak F (2001) Hyper-osmotic stress induces volume change and calcium transients in chondrocytes by transmembrane, phospholipid, and G-protein pathways. *J Biomech* 34(12):1527–1535.
53. Ohashi T, Hagiwara M, Bader DL, Knight MM (2006) Intracellular mechanics and mechanotransduction associated with chondrocyte deformation during pipette aspiration. *Biorheology* 43(3–4):201–214.
54. D'Andrea P, Vittur F (1997) Propagation of intercellular Ca2+ waves in mechanically stimulated articular chondrocytes. *FEBS Lett* 400(1):58–64.
55. Barrett-Jolley R, Lewis R, Fallman R, Mobasheri A (2010) The emerging chondrocyte channelome. *Front Physiol* 1:135.
56. Sánchez JC, Powell T, Staines HM, Wilkins RJ (2006) Electrophysiological demonstration of voltage-activated H+ channels in bovine articular chondrocytes. *Cell Physiol Biochem* 18(1–3):85–90.
57. Martins RP, Finan JD, Guilak F, Lee DA (2012) Mechanical regulation of nuclear structure and function. *Annu Rev Biomed Eng* 14:431–455.
58. Perera PM, et al. (2010) Mechanical signals control SOX-9, VEGF, and c-Myc expression and cell proliferation during inflammation via integrin-linked kinase, B-Raf, and ERK1/2-dependent signaling in articular chondrocytes. *Arthritis Res Ther* 12(3):R106.
59. Spiteri C, Raizman I, Pilliar RM, Kandel RA (2010) Matrix accumulation by articular chondrocytes during mechanical stimulation is influenced by integrin-mediated cell spreading. *J Biomed Mater Res A* 94(1):122–129.
60. Mathieu PS, Loboa EG (2012) Cytoskeletal and focal adhesion influences on mesenchymal stem cell shape, mechanical properties, and differentiation down osteogenic, adipogenic, and chondrogenic pathways. *Tissue Eng Part B Rev* 18(6):436–444.
61. Vincent TL (2013) Targeting mechanotransduction pathways in osteoarthritis: A focus on the pericellular matrix. *Curr Opin Pharmacol* 13(3):449–454.
62. Amin AK, Huntley JS, Bush PG, Simpson AH, Hall AC (2009) Chondrocyte death in mechanically injured articular cartilage—the influence of extracellular calcium. *J Orthop Res* 27(6):778–784.
63. Hu W, et al. (2012) Blockade of acid-sensing ion channels protects articular chondrocytes from acid-induced apoptotic injury. *Inflammation Res* 61(4):327–335.
64. Huser CA, Davies ME (2007) Calcium signaling leads to mitochondrial depolarization in impact-induced chondrocyte death in equine articular cartilage explants. *Arthritis Rheum* 56(7):2322–2334.
65. Rong C, et al. (2012) Inhibition of acid-sensing ion channels by amiloride protects rat articular chondrocytes from acid-induced apoptosis via a mitochondrial-mediated pathway. *Cell Biol Int* 36(7):635–641.
66. Liu YW, et al. (2011) Differential curvature sensing and generating activities of dynamin isoforms provide opportunities for tissue-specific regulation. *Proc Natl Acad Sci USA* 108(26):E234–E242.
67. Roux A, et al. (2010) Membrane curvature controls dynamin polymerization. *Proc Natl Acad Sci USA* 107(9):4141–4146.
68. Wiejak J, Wyroba E (2002) Dynamin: Characteristics, mechanism of action and function. *Cell Mol Biol Lett* 7(4):1073–1080.
69. Sauter E, Buckwalter JA, McKinley TO, Martin JA (2012) Cytoskeletal dissolution blocks oxidant release and cell death in injured cartilage. *J Orthop Res* 30(4):593–598.
70. Phillips DM, Haut RC (2004) The use of a non-ionic surfactant (P188) to save chondrocytes from necrosis following impact loading of chondral explants. *J Orthop Res* 22(5):1135–1142.
71. Kockskämper J, et al. (2008) The slow force response to stretch in atrial and ventricular myocardium from human heart: Functional relevance and subcellular mechanisms. *Prog Biophys Mol Biol* 97(2–3):250–267.
72. Bode F, Sachs F, Franz MR (2001) Tarantula peptide inhibits atrial fibrillation. *Nature* 409(6816):35–36.
73. Leddy HA, et al. (2014) Follistatin in chondrocytes: The link between TRPV4 channelopathies and skeletal malformations. *FASEB J* 28(6):2525–2537.
74. Liedtke W, et al. (2000) Vanilloid receptor-related osmotically activated channel (VR-OAC), a candidate vertebrate osmoreceptor. *Cell* 103(3):525–535.
75. Chen Y, et al. (2013) Temporomandibular joint pain: A critical role for Trpv4 in the trigeminal ganglion. *Pain* 154(8):1295–1304.
76. Guilak F, Erickson GR, Ting-Beall HP (2002) The effects of osmotic stress on the viscoelastic and physical properties of articular chondrocytes. *Biophys J* 82(2):720–727.
77. Li J, et al. (2011) TRPV4-mediated calcium influx into human bronchial epithelia upon exposure to diesel exhaust particles. *Environ Health Perspect* 119(6):784–793.
78. Yeo M, Berglund K, Augustine G, Liedtke W (2009) Novel repression of Kcc2 transcription by REST-RE-1 controls developmental switch in neuronal chloride. *J Neurosci* 29(46):14652–14662.
79. Schmittgen TD, Livak KJ (2008) Analyzing real-time PCR data by the comparative C(T) method. *Nat Protoc* 3(6):1101–1108.
80. Coste B, et al. (2012) Piezo proteins are pore-forming subunits of mechanically activated channels. *Nature* 483(7388):176–181.
81. Suchyna TM, et al. (2004) Bilayer-dependent inhibition of mechanosensitive channels by neuroactive peptide enantiomers. *Nature* 430(6996):235–240.
82. Amin AK, et al. (2011) Hyperosmolarity protects chondrocytes from mechanical injury in human articular cartilage: An experimental report. *J Bone Joint Surg Br* 93(2): 277–284.